

Expanded View Figures

Figure EV1. Characterization of Yb body components.

- A Western blotting was performed using anti-SoYb and anti-Vret monoclonal antibodies produced in this study. β -tubulin is shown as a loading control.
- B Subcellular localization of GFP-Shu and Shu-GFP transiently expressed in OSCs by transfection. Nuclei are shown in blue. Scale bar: 5 μ m.
- C Western blotting shows the levels of Yb body protein components in OSCs upon depletion of each component (kd). β -tubulin is shown as a loading control.
- D Immunofluorescence analysis shows Yb, SoYb, and Vret colocalized to Yb bodies. Colocalization of Armi with Yb was previously shown [16]. Nuclei are shown in blue. Scale bar: 5 μ m.
- E Immunofluorescence analysis in Shu kd OSCs. Yb, Armi, SoYb, and Vret were detected at Yb bodies upon Shu depletion. Nuclei are shown in blue. Scale bar: 5 μ m. The level of *Shu* mRNAs in Shu kd OSCs is shown on the right. Bars and error bars represent means \pm SEM values of three independent experiments. *P* value was calculated by *t*-test. ****P* < 0.001.

Source data are available online for this figure.

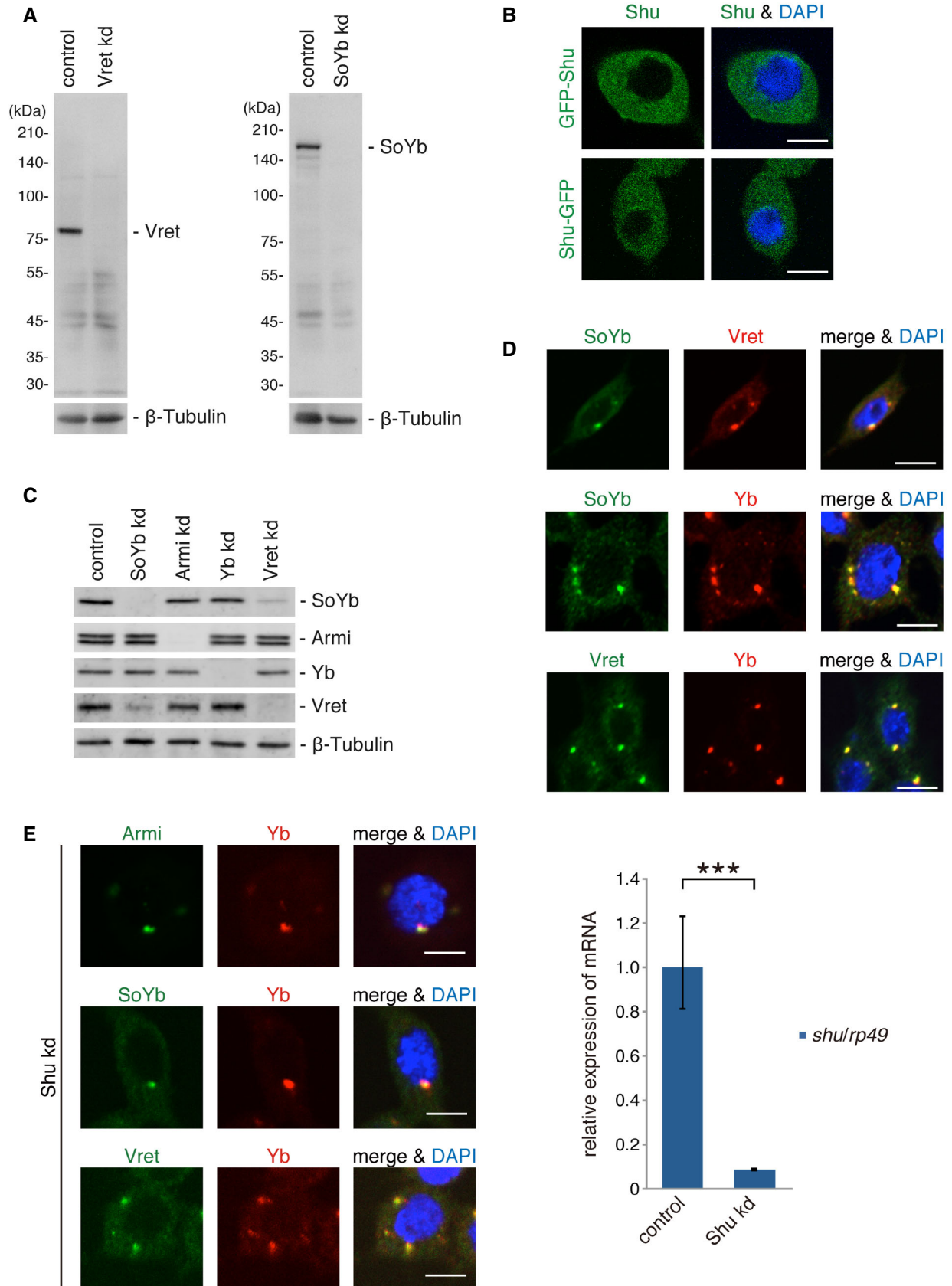


Figure EV1.

A

Yb protein

1 MEPIGDLQVP SFKVVSGGTT FTYASPKSGA ASLDFLAHTL RKREANTEKT ILICQQNFEA
61 ERLKFELAER DVNTILLPPH GAMVGQVLLL WSKGYINQAL IICDGMLEHL GVVEANLVIH Hel-C
121 TTLPELNKFE ERLKWLSISA RNAEMLVITP CDEENEKECK GETEPEIVQO RMPLKVDALN
181 SMOLYEIKEN TPPTSSSEDYK AEADVLLSAA TPATIPNDNK EQEINLSVED ATVKLLASFE
241 LGSTDSAAVD ESSPAAAKFN APVYSPFVTE NPTKSLDAEF OELVKSFKVO NVFKNMNLPP
301 PPSVSIEEPV SSASASDYRH QIDTTSLDSI RTVKDSPAASL AVVPFSAGGI TYNNYGVLGW
361 SRHAVVPCYG LTEAPDISTI IRRAMQOMGV ARSRARAVQR FAWPHVSLGK SVLVVGNLQI
421 GKTWSYLPTV CQRSHEDLQR RPDVGRGPTC IFVCPNQGG KQIERWMSTL LCLLGSASGF
481 EDVVTHTWDKT QLVDIVRRLK KPVGILLTSV DLLLQLLNHN PVGSIFDAQA VKCIALDNLN RNA helicase
541 DMVRVLPNDT MKLLQRLPEM FQLTQNKQCL LVSGRHWHTD LMVQHILPLM PDVLVLFDDA
601 LEASVYGGVQ LDVRVVADEP EKIEHLKALI AERRNFANEP AVMVCNSNTE VLLLRSLQA
661 IGVNAHICVS EACYSNVAEW LRQSPSGLLL VTDDVVPRLK CGKIPLLIHY SFASMWARFK
721 NRFSLFYANL KSPTTRPVGQ SVVFAKPTDL ENIWKLCDFY MKHKLPRPGH LLGILSQRRL
781 EEQPTSRSLC HQMAAFGDCL RHKCMYRHVM WRDEVLPDPH YPKNGLIRFL VLVCYSPAAL
841 AVRLSDQFPT AIRFLNFPMS DLGERVQRHY ELEANRHMHP NPVPGEMAVV KNINRYERVH eTud
901 IVSVESNMVM LVQLLDTSTE CFSYKTSQLY SCDKIFKDSP REAMDLRILG LQPESLDRIV
961 PDDARNLVRK DFFRRTHNKR NRQFHAVVQS AIHRTIFVRN IYDDEGNDLL SFVINRFRSH
1021 QDECCQLKLD AMVMSSKDCP YM 1042

B

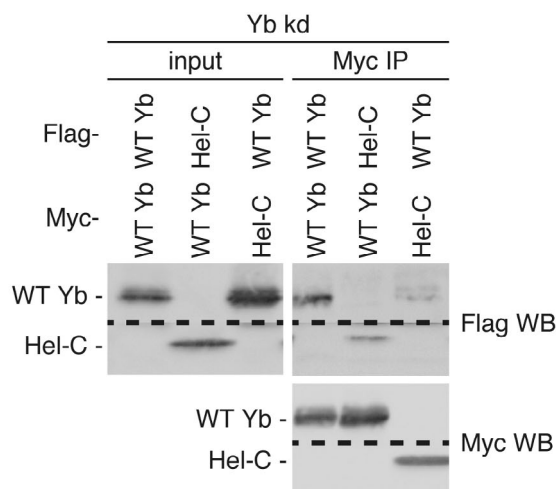


Figure EV2. Characterization of Yb.

A Amino acid sequence of Yb (CG2706). The Hel-C, RNA helicase, and eTud domains are indicated in orange, light blue, and dark blue colors, respectively. The potential IDR (for detail, see Fig EV3D) is underlined with a dotted line. Two residues, Gln399 and Asp537, which were mutated to alanine in Ref. [12], are underlined with blue bars.

B WT Yb associates with the Hel-C domain *in vivo*.

Source data are available online for this figure.

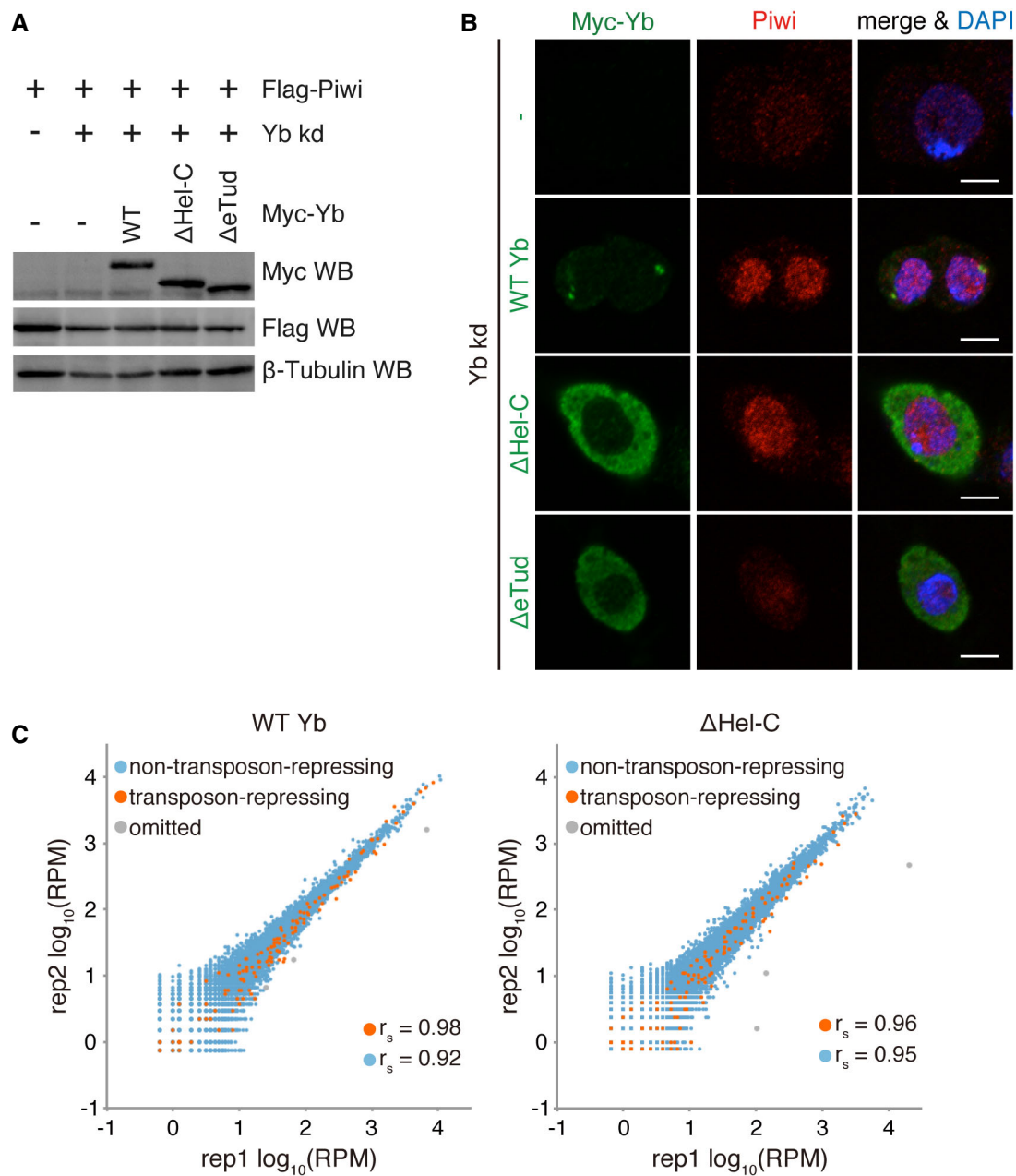


Figure EV3. Yb bodies are unnecessary for producing non-transposon-repressing genic piRNAs.

A Western blotting shows the levels of WT Yb and mutants expressed in the cells in Fig 3A.

B Immunofluorescence analysis showing that the expression of Δ Hel-C restored nuclear localization of endogenous Piwi in Yb-depleted OSCs. Nuclei are shown in blue. Scale bar: 5 μ m.

C Scatterplots showing reproducibility of piRNA-seq. Orange and blue dots indicate the number of normalized piRNA reads mapped uniquely to transposons in the reverse orientation and coding genes in the sense orientation, respectively. Three genes with low reproducibility (shown in gray) were omitted from further analysis.

Source data are available online for this figure.

Figure EV4. Yb bodies show characteristics of phase separation.

- A PONDR-FIT shows a potential IDR in Yb.
- B Amino acid sequence alignment of the N-terminal region of Yb in *D. melanogaster* (CG2076), *D. simulans* (JX64703.1), *D. yakuba* (XP_002100225), and *D. ananassae* (XP_001965435). The Hel-C domain is indicated in orange. Amino acid residues conserved among four *Drosophila* members are highlighted in blue. Tyr23 and Phe129 in Yb in *D. melanogaster* are shown by blue asterisks. The family tree of flies in the *D. melanogaster* group was adapted from Ref. [61].
- C Yb Y23A and F129A mutants barely interacted with WT Yb.
- D Yb Y23A and F129A mutants associated with Armi (left). Formation of Armi/SoYb/Vret complex was hardly affected by the mutants (right).
- E Proposed model for Yb body formation and piRNA biogenesis in OSCs. Homotypic Yb protein (light blue on left) binds *flam* RNA transcripts through their Yb binding sites (red bars). The Yb–Yb association and Yb–RNA interaction lead to the assembly of multivalent Yb bodies. Yb is shown in a trimer form for simplification, although it may multimerize *in vivo*. Yb bodies are often surrounded by mitochondria, on the surface of which piRNA biogenesis factors Zuc, Gasz, and Mino are present. At the interface of the two organelles (piRNA biogenesis site), *flam*-piRNA biogenesis occurs. Piwi bound to *flam*-piRNAs (Piwi-piRISC) is localized to the nucleus and silences transposons cotranscriptionally. Some piRNAs are produced independent of the Yb bodies. This happens when Yb lacks the Hel-C domain, leading to the failure of multivalent Yb body formation. Genic piRNAs may be produced in this way even in normal OSCs. *Flam*-piRNAs repress transposons but genic piRNAs are theoretically unable to target transposons. Piwi bound to genic piRNAs can also be localized to the nucleus, but is useless in transposon repression.

Source data are available online for this figure.

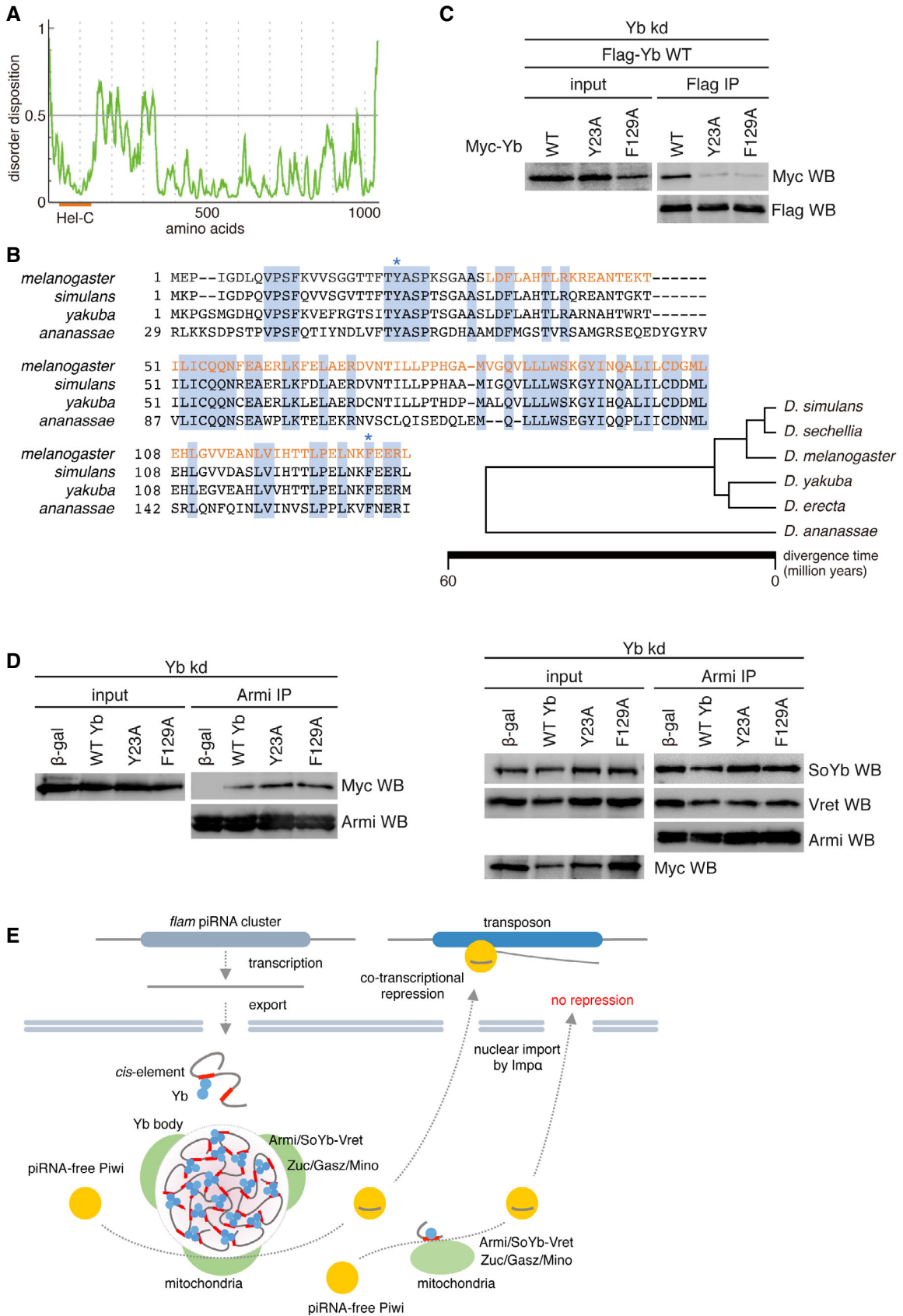


Figure EV4.